An Efficient Technique for Locating Multiple Narrow-Band Ultrasound Targets in Chorus Mode

Yongcai Wang, *Member, IEEE*, Lei Song, *Member, IEEE*, and S. S. Iyengar, *Fellow, IEEE*

***Abstract*—A basic problem in time of arrival (TOA)-based locating systems using narrow-band ultrasound (NBU) is how to improve the location update rate for tracking multiple targets. It is challenging because each ongoing ultrasound (US) signal occupies the channel for a rather long time because the slow propagation speed in air and it is hard to encode information in the narrow-band US. In this paper, we investigate to allow multiple NBU targets to transmit signals concurrently and to determine their locations by signal processing, which is called locating in *chorus mode*. The key observation is the signal interference characteristics of the concurrently chorusing targets. Based on it, the necessary and sufficient conditions for the receivers to determine the TOAs from multiple concurrently transmitting targets are investigated. However, because NBU cannot encode the target's ID, the detected TOAs are lacking labels of the target ID, causing ambiguities in location estimation. We exploited both *historical consistence* and *self-consistence* methods to narrow down the possible IDs of the TOAs and proposed *probabilistic particle filter algorithm* to disambiguate the motion trajectories of targets based on the targets' motion pattern consistency. A prototype of chorus-mode NBU locating system was developed. Extensive evaluations of both simulations and prototype experiments showed the effectiveness of the proposed theories and algorithms. In the testbed experiment, chorus locating provided 300% refreshing rate improvements compared with exclusive locating method, while the accuracy is still kept.**

***Index Terms*—Ultrasound locating, chorus mode, time of arrival, refreshing rate, multiple targets.**

I. Introduction

LOCATING by measuring time-of-arrival (TOA) of narrow-band ultrasound (NBU) has been widely used for accurately locating indoor targets. Its advantages include not only good positioning accuracy (in centimeter level), but also using very low cost hardware and simple system architecture. Therefore, it has attracted great research attentions and wide applications in the last two decades. e.g., ActiveBat [22], Cricket [14].

Manuscript received August 15, 2014; revised December 7, 2014; accepted January 11, 2015. Date of publication June 3, 2015; date of current version October 19, 2015. This work was supported in part by the National Natural Science Foundation of China under Grants 61202360, 61073174, 61033001, and 61061130540; by the Hi-Tech Research and Development Program of China under Grant 2006AA10Z216; by the National Basic Research Program of China under Grants 2011CBA00300 and 2011C-BA00302; and by NSF under Award 1158701.

Y. Wang and L. Song are with the Institute for Interdisciplinary Information Sciences, Tsinghua University, Beijing 100084, China (e-mail: wangyc@tsinghua.edu.cn; leisong03@gmail.com).

S. S. Iyengar is with the School of Computing and Information Sciences, Florida International University, Miami, FL 33174 USA (e-mail: iyengar@cis.fiu.edu).

Color versions of one or more of the figures in this paper are available online at http://ieeexplore.ieee.org.

Digital Object Identifier 10.1109/JSAC.2015.2441379

However, a long-standing challenge in using NBU-TOA-based indoor locating systems is *the low location refreshing rate for locating multiple targets*. This is because to avoid collision of NBU signals in the ultrasound channel, each transmitter (we consider targets are active to transmit signal) needs an exclusive time slot to transmit its signal. Because the ultrasound signal propagates slowly in air (around 340 m/s), each ongoing ultrasound (US) signal need to occupy the channel for nearly $t \approx 50$ ms. When there are multiple targets competing the channel, the location update rate for individual target is low, which also affects the tracking fidelity.

Previous studies investigated the multi-access locating problem by using broad-band ultrasound (BBU). It is because the broadband ultrasound signal can support Direct Sequence Spread Spectrum (DSSS) [8], [9] or Frequency Hoping Spread Spectrum (FHSS) [4], [5]. By modulating carrier signal with binary sequence, the broadband ultrasound can also encode the target ID information. But using broadband transducers will inevitably require higher hardware cost. Meanwhile, the broadband US signal is more sensitive to Doppler effects, which degrades the accuracy for locating quickly moving targets.

The focus of this work is on NBU-based locating system. It is hoped to preserve the advantages of NBU-based locating, i.e., low cost and robustness to target movement, while improving its multiple access locating capability as much as possible. Experiments motivated that even multiple NBU targets transmit simultaneously, only if their pair-wise distances to a receiver are big enough, the receiver can detected TOAs from these target efficiently. This motivates a *chorus mode locating*, in which some spatially distributed targets transmit US signals simultaneously while their locations are resolved concurrently by signal processing. The key is to investigate 1) the condition for successfully TOA detection from concurrently transmitted US signals; 2) the location-based transmission scheduling of the targets to satisfy above condition; 3) signal processing techniques to resolve the ambiguity to locate the targets. We investigated these problems in this paper.

1) At first, experiments and analysis are presented on the condition for a receiver to reliably separate multiple NBUs concurrently from multiple targets. It leads to the geometric conditions on concurrently transmitting targets for guaranteeing non-conflict, concurrent multiple TOA measurement.
2) Secondly, a transmission scheduling method for chorus mode locating is proposed. From initial state when target locations are unknown, targets are scheduled in greedy mode for multiple access, which improves locating updating rate greatly than existing exclusive mode.

3) Thirdly, since the measured TOAs are lack of source identity, both historical consistence (in terms of the deviation to the historical position of the targets) and self-consistence (in terms of the residue of location calculation) are exploited to narrow down the possible target IDs of the TOA.
4) At last, a probabilistic particle filter algorithm is introduced to further disambiguate the trajectories of the multiple targets by using the consistence of the moving speeds and accelerations of targets as the evaluation metrics.

We conducted both simulations and experimental testbed to verify the proposed theorem and algorithms. The rest of this paper is organized as follows. Related work and background are introduced in Section II. Problem and system setting is introduced in Section III. Characteristics of chorus locating are investigated in Section IV, with location-based transmitter scheduling presented in Section V. Algorithms for ambiguity resolving are presented in Section VI. Performance evaluation by simulations and hardware prototype are presented in Section VII. The paper is concluded with remarks in Section VIII.

II. Related Work and Background

Ultrasound TOA-based locating has attracted many research and application attentions.

A. TOA-Based NBU Locating Systems and Methods

NBU Locating Array: The seminal work for NBU TOA-based indoor locating system was proposed by Ward *et al.* [22] in 1997. They presented a Bat system, which tracked mobile NBU transmitters by an array of NBU beacons mounted on the ceiling. A RF controller connected to a computer synchronizes the beacons by periodical RF signal. The beacons detect TOAs from the mobile target for calculating target's location.

Distributed NBU Locating System: Later works presented distributed locating system instead of using beacon array. In Cricket [14] system presented by Priyantha *et al.*, each beacon is an individual node embedded with RF and US modules. Beacons can be deployed and calibrated as will. The target transmits RF+US together, in which the RF signal is used to synchronize the beacons within audible region. Then the synchronized beacons detect US to estimate TOAs from the transmitter for position calculation. Another distributed NBU locating system is Dolphin, developed by Minami *et al.* [12].

Auto-Calibration: Later, Zhao *et al.* presented AUITS [26], which addressed the autonomous beacon calibration problem. The presented system is composed by a fixed topology positioning device, so that the device can be placed anywhere to locate mobile targets without laborious calibration. Another auto-calibration algorithm was presented by Nishitani *et al.* [13].

TDOA-Based Locating for Navigation: A reversing way for target navigation is to let the beacons at fixed locations transmit NBU signals periodically. The targets worked as receivers to detect NBU and calculate their own locations by Time-Difference-Of-Arrival method [24]. Since NBU based locating systems can provide centimeter level positioning accuracy, it enables location context based applications, including location-based access control [21], location based advertising delivery [27], robot navigation [24], and sensor network security [17] etc.

Multiple Access: When NBU is used, existing approaches generally exploited Time Division Multiple Access (TDMA) method [22] to schedule the transmissions, or exploited the RF signal to detect concurrent transmission, which enabled Carrier Sense Multiple Access (CSMA). In CSMA-based scheduling the RF signal is used not only for synchronization, but also for collision avoidance and transmitter identification [14] [26]. In these traditional multiple access scheme, each ongoing NBU signal need to occupy an exclusive time slot during its propagation. Because of the slow speed of ultrasound in air, the location updating rate for individual target is low. Woodman *et al.* [23] proposed multiple radio zones scheduling method in the Bat system. Its difference to our work is that we address not only the multiple access problem but also the ambiguity resolving and the multiple target tracking problems.

B. Multiple Access in Broadband US Locating Systems

To enable multiple targets transmit concurrently, existing approaches exploited to use broadband ultrasound. Compared to the narrowband, broadband ultrasound requires the transducer [8] to have better frequency response performance. The broadband ultrasound wave can modulate target ID and if the US wave is encoded with orthogonal code [1], multiple waves can be decoded respectively even overlapped.

DSSS Multiple Access: Based on these advantages, Hazas *et al.* [8], [9] proposed broadband ultrasonic location system. They applied Direct Sequence Spread Spectrum (DSSS) to modulate transmitter ID by gold code. So that the system has multiple access property because the corruption due to signal collision is minimal. Villadangos *et al.* [19] used the similar DSSS multiple access technique, but used TDOA technique for location calculation, so that there is no need for synchronization among transmitters.

FHSS Multiple Access: Gonzalez *et al.* [5] proposed frequency hopped spread spectrum (FHSS) multiple access and used both TOA and AOA (Angle of Arrival) of ultrasound to estimate the location and orientation of the mobile targets. Saad *et al.* [16] further improved the robustness of FHSS based multiple access ultrasound locating. The presented a minimum variance search technique to correct the error in the cross-correlation time-of-flight estimation. Gonzalez *et al.* [4] compared the accuracy of FHSS-based and DSSS-based multiple access locating, and showed that FHSS-based locating method generally can have better accuracy for better noise tolerance. They also presented [6] piezoelectric bandwidth modification method to produce low cost broadband transmitters.

But using broadband ultrasound for target locating need broadband transducers, which cause the locating system more expensive. The system is also sensitive to the Doppler effects.

C. Chorus Mode Locating and Scheduling

To the best of our knowledge, very few results have been reported for locating using NBU in chorus mode. The major difficulty is how to resolve the signal collision and how to label the measured TOAs. A conference version of this work [18] reported the experiments results and the characteristics of the blind region. The idea of chorus mode locating is to fully

reuse the space for concurrent transmissions, which is similar to Spatial Time Division Multiple Access algorithms [2], [7], [25] in ad-hoc sensor networks. It also like spectrum detection problem for multiple channel scheduling [11]. But the difference in chorus locating is that, a transmitter needs to access at least $d+1$ non-collinear beacons for efficient locating, instead of accessing only one beacon, and the TOAs don't have ID labels.

III. Problem and System Setting

Inspired by existing works and requirement, we investigated chorus model locating. We firstly introduce the chorus locating problem and the system settings.

A. Problem Introduction

We consider M static beacons denoted by $\mathbf{B}$ are deployed in a d-diminutional space. The coordinates of these beacons are previously calibrated, which are denoted by $\mathbf{Z} = \{\mathbf{z}_1, \cdots, \mathbf{z}_M\}$, where $z_i \in \mathbb{R}^d$. Each beacon is integrated with a RF (radio frequency) and a US receiver. The RF is used for time synchronization and US module is for TOA detection. N mobile targets (denoted by $\mathbf{T}$) move in the sensing field of the beacons, whose real-time coordinates $\{\mathbf{x}_1(t), \cdots, \mathbf{x}_N(t)\}$ are the variables to be determined.

1) Exclusive Mode Locating: We firstly introduce the locating routine of exclusive mode. The locating routine involves *ranging* and *locating* two steps.

Ranging: In exclusive mode, each target emits RF (radio frequency)+NBU signals simultaneously in an exclusive time slot without interfering other targets. Consider a target i is transmitting. The beacons detect RF from i to known its target ID and start time counters. The time counters are stopped after detecting the rising edge of the successive US wave(if the strength of the received US wave is higher than a threshold). Then the *Time-Of-Arrival (TOA)* of US from target i to each audible receiver j is measured, which is then multiplied by the ultrasound speed in air to infer the beacon-target distance, denoted by $D_{i,j}$.

Locating: When more than $d+1$ distances from non-collinear beacons are measured, the location of the target is calculated by trilateration [26] or least square estimation (LSE) [14].

2) Chorus Mode Locating: In contrast to the exclusive mode, in chorus mode, multiple targets are allowed to broadcast NBUs concurrently. A *RF commander* is used to broad RF to synchronize both targets and receivers. A scheduling scheme is applied to let a set of k spatially well separated targets to broadcast NBU signals at the same time. Then, each receiver detects a sequence of rising edges from the received NBU wave, which constitute n_j anonymous distance measurements at beacon j, denoted by $\mathbf{D}_j(t)$. Note that $n_j \leq k$ is the number of TOA detected by beacon j. Then the location algorithm takes the anonymous distance measurements from the beacons $[D_1(t), \cdots, D_M(t)]$ as input, and utilizes the coordinates of the beacons $[\mathbf{z}_1, \cdots, \mathbf{z}_M]$ to infer the real-time locations of the k transmitting targets.

Since RF's communication radius is much larger than US, we assume all beacons can be synchronized by the RF commander.

TABLE I
List of the Major Notations

Notations	Description
$\mathbf{B}, \mathbf{z}$	Beacon set; Coordinates of beacons
$\mathbf{T}, \mathbf{x}(t)$	Target set; Realtime locations of targets at t
$T_i, \mathbf{x}_i(t)$	Target i, and location of target i at t
$D_{i,j}$	Measured distance from target i to beacon j
$\mathbf{D}_j$	Anonymous distance set measured by beacon j
n_j	Number of measured distance by beacon j
r	Radius for US TOA detection
v_u	Ultrasound speed in air
$v_i(t)$	Moving speed of target i at t
v_e	Target velocity upper bound
ω	confident separation distance for wave peak detection
$\mathbf{C}$	concurrently transmitting target set
d_s	Separation distance between concurrently transmitting targets.
$d_{a,b}$	Distance between target a and target b
$S^B_{a \leftarrow b}$	Blind region of target a interfered by target b
$S^D_{T_i \leftarrow \mathbf{C}_i}$	Detectable region of T_i at the interference of targets in $\mathbf{C}_i$
$\mathbb{T}_i(1:t)$	Trajectory of target i from 1 to t
$p_v(x)$	probability density function of velocity
$p_a(x)$	probability density function of acceleration

The audible radius of US is denoted by r. We consider the environment is open where the NLOS problems are not serious. We discussed how to deal with US echoes in Section IV.

B. System Setting

Therefore the system is composed by M beacons, N mobile targets, and a RF commander for beacon synchronization and target scheduling. All the beacons and targets are integrated with RF+US transducers. At time t, the RF commander broadcasts transmission scheduling to the targets. When targets receive the command, some of them broadcast US follow the scheduling. When the receivers receive the command, they start time counter synchronously. Distances measured by receivers are sent to a server, where the locations of the transmitting targets are updated. The main notations used in this paper are listed in Table I.

IV. Characteristics Investigation

A. Experimental Investigation

Detecting TOAs from concurrently transmitted NBU waves at the receiver is the first step for chorus locating. We conducted experiments using MTS450CA Cricket nodes [14] to investigate the conditions for measuring multiple TOAs from concurrent transmitters.

Before carrying out the experiments, we made some modification to the firmware of Cricket node. Firstly, the policy on beacon to detect only the first arising edge was canceled. We customized the firmware, so that every rising edge over the threshold is detected and the TOA is obtained correspondingly. Secondly, the CSMA protocol was disabled, so that the targets can send ultrasound simultaneously.

1) Aftershock: In the first experiment, one receiver and one target are used. The screen-shot on oscilloscope is shown in Fig. 1(a). The target's NBU has length 200 μs. After about 4 ms, this NBU arrives at the receiver, which cause a 1 ms shock on the receiver's transducer. Because the ultrasound is mechanical

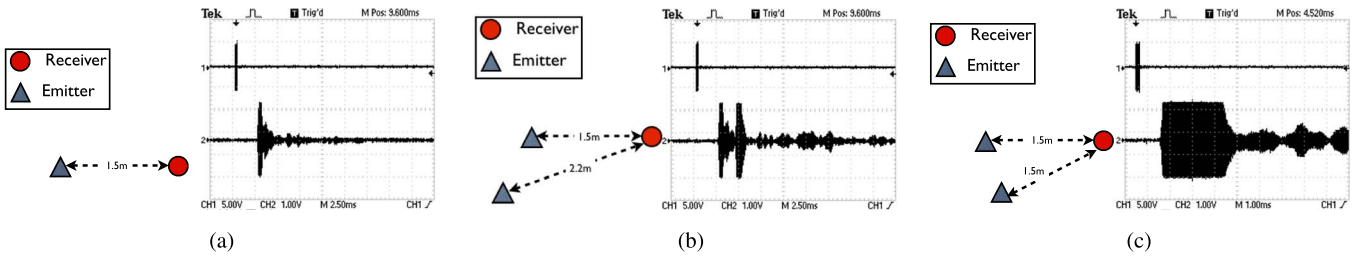

(a) (b) (c)

Fig. 1. Experiments to test how the separation of NBU peaks is affected by the distances between the transmitters. (a) one target, one receiver. (b) two targets have different distances to the receiver. (c) two targets have the same distance to the receiver.

wave, the shocking on the receiver is much longer than the length of the wave sent by the target. This phenomenon is called *aftershock*. When the sensor in the receiver is experiencing an aftershock, the comparator in the sensor is kept in *high state*, which will block the detection of the newly arrived NBU wavefront. From the oscilloscope output, we can also see some secondary peaks caused by the echoes. These secondary peaks can be filtered out because their powers are lower than the threshold. After the energy of the aftershock fades below the threshold, the comparator switches to *low state*, which is ready for detecting the next NBU wave.

2) Multiple TOA Detections: Two targets and one receiver are used in the second experiment, in which targets' distances to the receiver differs by 0.7 m. When the two targets transmit US signal simultaneously, the detected waves at the receiver are shown in Fig. 1(b). Two NBU riding edges are detected which indicate TOAs from two targets. But note that the detected TOAs are anonymous, i.e., the receiver don't know the target ID of the TOA.

In the third experiments, the two targets are placed at the same distance to the receiver. The captured US waves at the receiver are shown in Fig. 1(c). We can see only one rising edge. This is because the difference of two waves' arriving times is shorter than the first wave's aftershock. In this case, only one TOA can be detected whose source ID cannot be known.

B. Extract the Multiple TOA Detection Condition

The experiments showed that whether two successive NBU waves arrived at a receiver could be successfully detected was determined by the time separation between the two arrived US waves. If the time separation is longer than the length of the aftershock generated by the first wave, the rising edge of the second wave can be detected. Since the length of the aftershock is affected by the received energy of the NBU signal and the character of US sensor, it will be better to choose ultrasound transducer with weak inertia and shorter aftershock. To formulate the impact of the aftershock, let's denote L_{max} be the longest possible aftershock generated by the first wave at the receivers. Let v_u be the speed of the ultrasound, then

Definition 1 (Confident Separation Distance): We define $\omega = L_{max} v_u$ as the confident separation distance.

L_{max} indicates the time separation for detecting two wave fronts successfully. ω turns this separation requirement to the distance separation. If two targets' distances to a receiver (in their sensing range) differ more than ω, the receiver can detect two unlabeled TOAs in case the two targets transmit simultaneously.

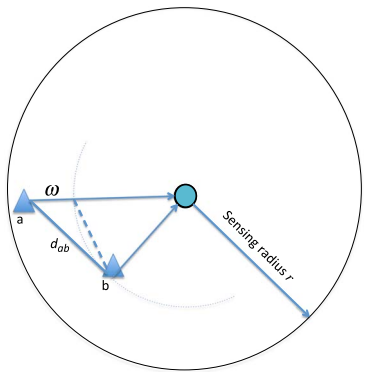

Fig. 2. Triangle inequality relationship.

From triangle inequality as shown in Fig. 2, if the distance from two targets to a receiver differs more than ω, the distance between the two targets must be larger than ω. Let's further take the audible region of the receiver into consideration. Let audible radius r be the maximum propagation distance of BNU before its strength is lower than the detecting threshold. By combining the separation distance with the audible range, we can get the following multiple TOA detection condition:

Theorem 1 (Multiple TOA Detection): We consider two targets a and b are at location $\mathbf{x}_a$ and $\mathbf{x}_b$ respectively, which send NBU waves concurrently. One receiver at location $\mathbf{z}_x$ can detect the TOAs from the two targets if:

$$\begin{cases} |d_{a,x} - d_{b,x}| > \omega \\ D_{a,x} \leqslant r, D_{b,x} \leqslant r \end{cases} \tag{1}$$

where $d_{i,j}$ is the distance between $\mathbf{x}_i$ and $\mathbf{x}_j$; $D_{a,x}$ is the distance from target a to beacon x.

For multiple-target transmitting case, we only need to consider the targets in the audible region of each receiver. To check whether a receiver can detect TOAs from the concurrently transmitting targets, we can simply sort their distances to the receiver in ascending order $\{d_1 \leq d_2 \leq \cdots d_n\}$. If $\forall i = 1, \cdots, n-1, d_{i+1} - d_i > \omega$, then the receiver can successfully detect the TOAs of signals from all these targets.

C. "Blind Region" Impacted by Concurrent Targets

Let's consider a more complex problem when there are multiple receivers want to track multiple transmitters. We firstly

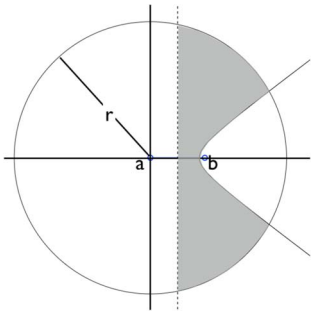

Fig. 3. The blind region of a caused by b.

consider in which region can receivers detect TOA from a when another target b is transmitting concurrently. We investigate this problem in 2-D space, which has the same principle in 3-D space.

Definition 2 (Blind Region): Blind region of target a caused by target b is a subregion in the audible region of a, in which the receivers cannot detect TOA from a when a and b transmit concurrently. The blind region of a caused by b is denoted by $S^B_{a\leftarrow b}$.

Let (x, y) be an arbitrary coordinate in the 2-D space, representing the location of a receiver, for two targets a and b at location (x_a, y_a) and (x_b, y_b), the functions $|d_{a,x} - d_{b,x}| = 0$ $|d_{a,x} - d_{b,x}| = \omega$ partitions the audible region of a in the 2-D space into three subregions. The blind region $S^B_{a\leftarrow b}$ is characterized by the mid-perpendicular between (x_a, y_a) and (x_b, y_b) and the hyperbola: $|d_{a,x} - d_{b,x}| = \omega$.

In Fig. 3, the blind region $S^B_{a\leftarrow b}$ is shown in grey color. Receivers in this region cannot detect TOA from a because the interference from b. Depending on the distance between a and b, the area of $S^B_{a\leftarrow b}$ varies from 0 to $\frac{\pi r^2}{2}$. Fig. 4 shows how $S^B_{a\leftarrow b}$ changes with $d_{a,b}$. The area of blind-region can be expressed in close form as a function of $d_{a,b}$.

$$S^B_{a\leftarrow b}(d_{a,b}) = \begin{cases} 0 & d_{a,b} > 2r \\ r^2(\theta - \sin\theta\cos\theta) & 2r - \omega \le d_{a,b} \le 2r \\ r^2(\theta - \sin\theta\cos\theta) - S_e & \omega < d_{a,b} < 2r - \omega \\ r^2(\theta - \sin\theta\cos\theta) & 0 < d_{a,b} \le \omega. \end{cases} \tag{2}$$

The detailed expansion of $S^B_{a\leftarrow b}(d_{a,b})$ can be referred in Appendix A. We should note that the area of $S^B_{a\leftarrow b}$ is a monotone decreasing function of $d_{a,b}$. The smaller is $d_{a,b}$, the larger is the blind region. Now, let's consider the TOA-detectable region when there are multiple concurrently transmitting targets.

Definition 3 (TOA Detectable Region (TDR)): Let a k targets $T_1, \cdots, T_k$ transmit concurrently. Let set $\mathbf{C}_i$=$\{T_1, \cdots, T_j, \cdots, T_k\}(j \neq i)$ be the concurrently transmitting targets except T_i. Denote the TOA detectable region of target T_i at the interference of $\mathbf{C}_i$ by $S^D_{T_i\leftarrow\mathbf{C}_i}$. Then $S^D_{T_i\leftarrow\mathbf{C}_i} = S^A_{T_i} \setminus \cup_{s\in\mathbf{C}_i} S^B_{T_i\leftarrow s}$, which is the audible region of T_i subtract the blind regions caused by other concurrent transmitting targets.

D. Lower Bound of TOA Detectable Region (TDR)

In d-dimension space, for locating a target, TOA measurements from more than $d + 1$ non-collinear beacons are needed for trilateration. If Least Square Estimation is used, more number of TOA are involved in calculation can reduce the location variance. Therefore, an intuition for locating target accurately in chorus mode is to make sure the *TOA detectable region (TDR)* of a target be big enough, so that more non-blind beacons can be accommodated to contribute enough TOA measurements.

Therefore, in this subsection, we characterize a lower bound of $S^D_{T_i\leftarrow\mathbf{C}_i}$ when the pairwise distances among the concurrently transmitting targets are larger than a *minimum pairwise distance* d_s. The minimum pairwise distance exists because the fact that in real applications, the concurrently transmitting targets are scattered in the monitoring field. We can also schedule based on the targets' locations to make the concurrent transmitters well serrated (will be introduced soon). Based on it, the lower bound of $S^D_{T_i\leftarrow\mathbf{C}_i}$, which is a function of k, d_s and r will provide guidelines for target transmission scheduling in the chorus mode locating.

Theorem 2 (Most Interfering Target Distribution): When $k - 1$ interfering targets with minimum pairwise distance d_s are presenting, the $k - 1$ targets generate the largest blind region to a when they are located on the circle centered at a, with radius d_s, and separated by angle $\frac{2\pi}{k-1}$, i.e., evenly distributed on the circle with radius d_s around a.

Proof 1: First, since $S^B_{a\leftarrow s}$ is a monotone decreasing function of the distance between a and s. $\forall s = \{T_1, \cdots, T_k, s \neq a\}$, $S^B_{a\leftarrow s}$ is the largest when $d_{a,s}$ is the minimum, i.e., $d_{a,s} = d_s$. Secondly, we prove the overlapping area of the blind regions are largest when other targets are evenly separated on the circle around T_i with radius d_s. We treat the problem as a set cover problem. The audible region of a can be thought as a whole set containing infinite points. $S^B_{a\leftarrow s}$ is a covering subset and the $k - 1$ covering subsets are isotropic, i.e., with the same size and the same shape. By inclusion-exclusion principle, the union of the most exclusive subsets will contribute the largest cover to the whole set. The subsets are most exclusive when the $k - 1$ targets are evenly separated on the circle around T_i.

Fig. 5 shows the maximum union area of the blind regions of a when $|T| = 2, 3, 4, 5, 6$ respectively. Other targets generates the maximum blind region to a when they are symmetrically distributed on the circle around a with radius d_s. The area of $S^D_{a\leftarrow\mathbf{C}_i}$ reaches the lower bound in such case, which affects the possible number of non-blind beacons in it.

More generally, when the number of concurrently transmitting target, i.e., k is unknown and the target distribution is arbitrary, we can also derive a lower bound for $S^D_{a\leftarrow\mathbf{C}_i}$ only if d_s is given.

Theorem 3 (General Lower Bound of $S^D_{a\leftarrow\mathbf{C}_i}$): The lower bound of $S^D_{a\leftarrow\mathbf{C}_i}$ for given pairwise separation d_s is:

$$S^D_{a\leftarrow\mathbf{C}_i} \ge \pi\left(\frac{d_s}{2}\right)^2 \tag{3}$$

Proof 2: From (2), the inscribed circle centered at a with radius $d_s/2$ must not be in the blind region generated by any other target. So the circle area with radius $d_s/2$ must be in the TDR. Its area gives lower bound to $S^D_{a\leftarrow\mathbf{C}_i}$ as shown in Fig. 6.

We can see the lower bound is a monotone increasing function of d_s, which means that the larger is the pair-wise

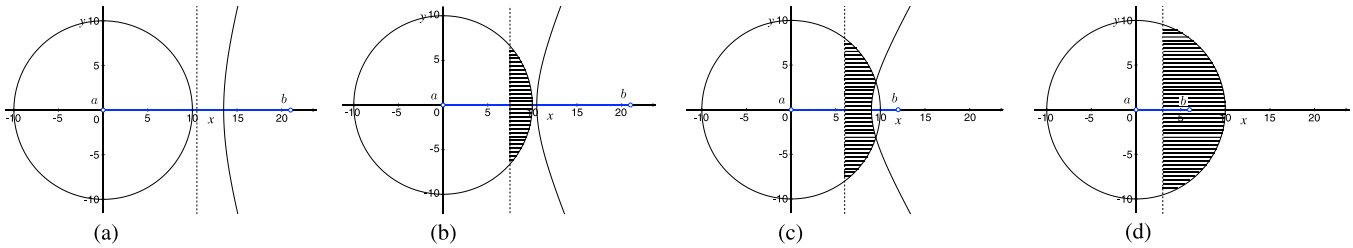

Fig. 4. The grey region stands for blind region, where the rest part in audible-circle is audible region. (a) $d_{a,b} > 2r$. (b) $2r - \omega \leq d_{a,b} \leq 2r$. (c) $\omega < d_{a,b} < 2r - \omega$. (d) $0 < d_{a,b} \leq \omega$.

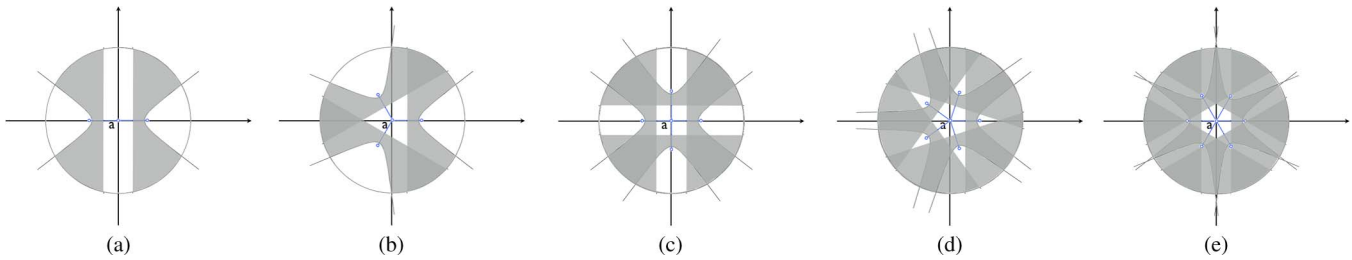

Fig. 5. Blind-region of target a caused by different number of other targets. (a) Blind region by 2 targets. (b) by 3 targets. (c) by 4 targets. (d) by 5 targets. (e) by 6 targets.

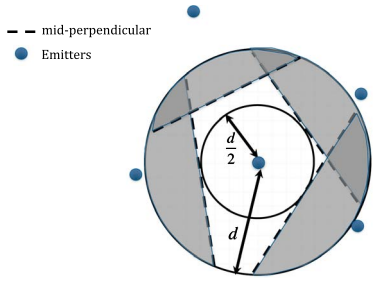

Fig. 6. Lower bound of blind-region.

separation among the targets, the larger is the area of TDR for a target.

E. Probability of Having at Least Three Beacons in TDR

Consider in 2D space, TOA measurements from three non-collinear beacons are needed for trilateration. Based on the lower bound of $S^D_{a\leftarrow \mathbf{C}_i}$, for any given distribution of the beacons, we can evaluate the probability and the expectation of at least three beacons in the TDR region of a target. The probability can guide the transmitter scheduling scheme to choose proper d_s for achieving good target tracking performances.

Let's consider a general case when the receivers are in Poisson distribution, i.e. $P(n_r = k) = \frac{\lambda^k e^{-\lambda}}{k!}$, where λ is the expected number of receivers in a unit area (e.g. 1 m^2). By substituting the lower bound of $S^D_{a\leftarrow T} \geq \pi \left(\frac{d_s}{2}\right)^2$, the probability of at least three receivers are in $S^D_{a\leftarrow T}$ can be calculated as:

$$1 - \sum_{i=0}^{2} p(n_r = i) \geq 1 - e^{-\frac{\lambda\pi d_s^2}{2}} \left[1 + \frac{\lambda\pi d_s^2}{2} + \frac{\lambda^2\pi^2 d_s^4}{8}\right] \quad (4)$$

Theorem 4: When receivers are in Poisson distribution with λ expected receivers in a unit area, when the pair-wise separation among targets are larger than d_s, the probability of at least three receivers are presenting in the TDR of a target is lower bounded by

$$1 - e^{-\frac{\lambda\pi d_s^2}{2}} \left[1 + \frac{\lambda\pi d_s^2}{2} + \frac{\lambda^2\pi^2 d_s^4}{8}\right]. \quad (5)$$

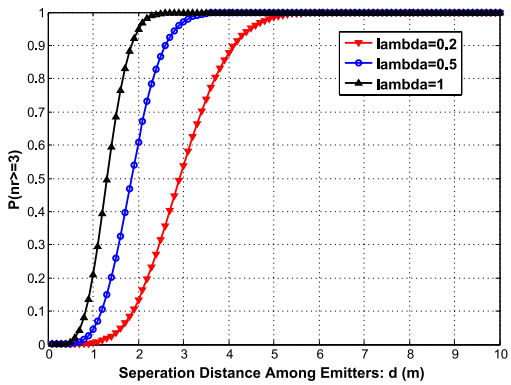

Fig. 7. Probability of three receivers are in TDR.

Fig. 7 plots the lower bound of $P(n_r \geq 3)$ as a function of d_s and λ. We can see that for given λ, the lower bound of at least three receivers presenting in the TDR of a target increases exponentially with d_s. Note that the figure plots only the lower bound. Because the real TDR area can be much larger than the lower bound area of TDR, in real case, the probability of three receivers are in the TDR of a target can be much closer to 1.

The results in Fig. 7 show the strong feasibility of chorus locating. Targets only need to be separated by 2 to 5 meters in case of different beacon deployment densities for obtaining at least three distance measurements for locating a mobile target.

V. Transmission Scheduling

The characteristics of the TDR area and the requirement of multiple TOA measurements for locating a target inspire a location-based transmission scheduling scheme. It starts from

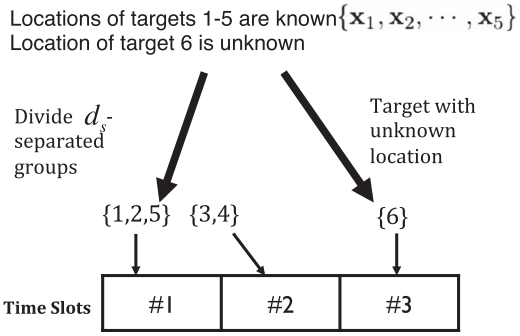

Fig. 8. An example of LBTA to assign time slots.

the initial state where each target transmits in exclusive time slot. When the targets' locations are known, targets are divided into several concurrent transmission groups. Targets in the same group transmit US concurrently. The schedule is conducted by a controller and is delivered to the targets by a RF messages.

The main idea is to let targets with enough pair-wise separation distances to transmit concurrently. A location based time-slot assignment (LBTA) algorithm was designed. It assigns exclusive time-slots to targets which are close to each other or with unknown locations, and let targets with known location transmit concurrently in a greedy manner.

At first in LBTA, a confident separation distance d_s is calculated by the lower bound of TDR region (5) based on the given density of the receivers to guarantee the probability of $P(n_r \geq 3)$ approaching 1. Then the targets with known locations will be separated into a set of *d_s-separated groups*. Each group consists of several d_s separated targets. Each group occupies an exclusive time slot and targets in the same group transmit together. Exclusive slots are assigned to the targets with unknown locations.

An example of LBTA is shown in Fig. 8, in which, six targets are presenting. We assume the locations of target $\{1, \ldots, 5\}$ are known and the locations of targets 6 is still unknown. In this case, the targets with known locations are separated into two *d_s-separated groups*. Totally three slots are assigned to the six targets.

Although finding the minimum number of d_s-separated group is NP-hard [3], this problem can be effectively addressed by a greedy approach in practice when the number of targets are limited. We proposed a greedy *DivideClosestTargets* algorithm to address it.

Algorithm 1 DivideClosestTargets

Require: $\{\mathbf{x}_1, \ldots, \mathbf{x}_N\}$ and d_s
Ensure: d_s-seperated group partition, $\mathcal{G}_1, \ldots, \mathcal{G}_{n_d}$
1: $n_d \leftarrow 1$, $\text{tempg}_1 \leftarrow \{\mathbf{x}_1, \ldots, \mathbf{x}_N\}$, $\text{tempg}_2 = \emptyset$
2: **while** $\cup_{i=1}^{n_d-1} \mathcal{G}_i \neq \{\mathbf{x}_1, \ldots, \mathbf{x}_N\}$ **do**
3: **while** (MinPairWiseDis($\text{temp}\mathcal{G}_1$) $< d_s$) **do**
4: $[i, j]$ = select the closest pair in tempg_1
5: $\text{temp}\mathcal{G}_1 = \text{temp}\mathcal{G}_1 \setminus i$, $\text{temp}\mathcal{G}_2 = \text{temp}\mathcal{G}_2 + i$
6: **end while**
7: $\mathcal{G}_{n_d} = \text{temp}\mathcal{G}_1$, $n_d = n_d + 1$
8: $\text{temp}\mathcal{G}_1 = \text{temp}\mathcal{G}_2$, $\text{temp}\mathcal{G}_2 = \emptyset$
9: **end while**

DivideClosestTargets always selects the closest pair in the current temp group, and put one of them into a new temp group, until all targets in current temp group have pairwise distance larger than d_s. This temp group will form a d_s-separated group. Then the algorithm process the new temp group, until all targets are assigned into d_s-separated groups. The scheduling on one hand improve the location updating rate for individual target, on the other hand helps to provide enough number of TOAs for locating each target in the chorus mode. When new targets entered the system, it registers itself to the scheduler by sending RF signal, so that the scheduler will assign slots to it for get it initial location and adds it into the later scheduling loops. When the ultrasound from a target has not been received for a long enough time, the scheduler judges the target has left and stops to assign time slot to it.

Based on the scheduling, beacons detect multiple TOAs from concurrently transmitting targets. The next step is how to determine the location of targets based on these anonymous TOAs.

VI. Resolving Ambiguity

To use these anonymous TOAs for locating mobile targets, we need to label each TOA by possible target IDs, so that to determine the location of the multiple targets.

What we can rely on is the spatial and temporal consistency of each target's movement, i.e., each target cannot jump suddenly. We present a framework to firstly narrow down the possible IDs of TOAs, and then disambiguate the trajectories of the multiple targets by probabilistic particle filter.

A. Algorithm Overview

Let the concurrently transmitting target set by $\mathbf{C}$. The input of the problem includes unlabeled TOA measurements at beacons and the historical locations of the targets in $\mathbf{C}$. Note that the targets' historical locations have been available when the targets turn to the chorus locating mode.

Problem 1 (Chorus Locating Problem): Let's define a round as a period in which all targets can finish location updating. Then in round t, the problem inputs include (1) Anonymous distances measured by the beacons at round t, denoted by $[\mathbf{D}_1(t), \cdots, \mathbf{D}_M(t)]$; (2) Coordinates of these beacons, denoted by $[\mathbf{z}_1, \cdots, \mathbf{z}_M]$, (3) The historical positions of the concurrently transmitting targets, denoted by $\{\mathbf{x}_i(t-1), i \in \mathbf{C}\}$. The problem output is to determine the real-time locations of the targets in $\mathbf{C}$ at a round t.

To address this problem, the overview of the proposed techniques are shown in Fig. 9, which contain mainly two parts: 1) consistent position generation and 2) probabilistic particle filter for trajectory disaggregation.

1) Overview of Consistent Position Generation: Every $d+1$ distances from non-collinear beacons can generate a position candidate. Enumerating the combinations of the anonymous distances will generate a large amount of possible positions. To narrow down the potential positions, we firstly proposed to reject the infeasible distance groups by *historical-consistency*, i.e., by utilizing the consistency of distance measurements with the latest location estimations of the targets. After this step, the distance groups are utilized to generate a set of potential

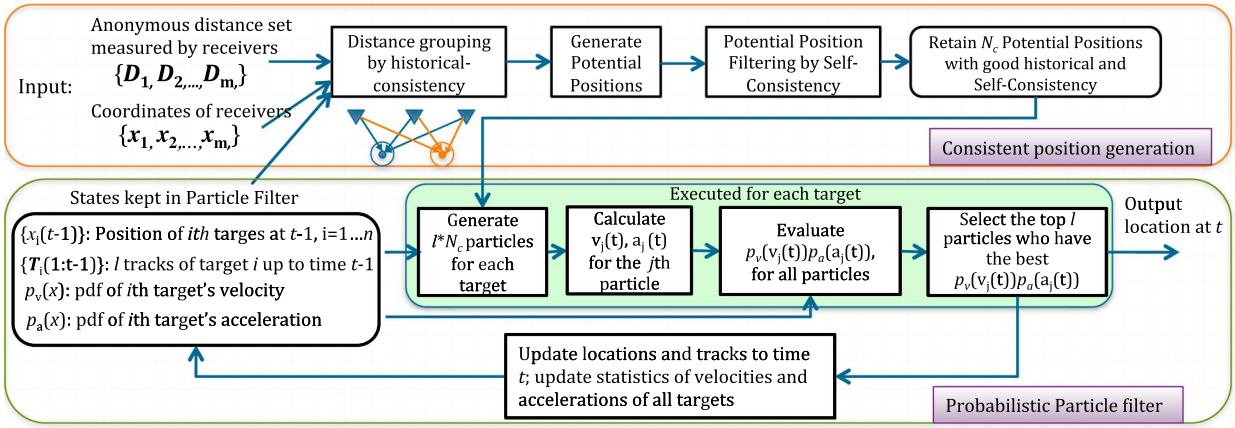

Fig. 9. The diagram of consistent location generation and probabilistic particle filter algorithms to utilize the anonymous distances measured by receivers to locate and disambiguate the tracks of multiple targets.

positions. To further narrow down the potential positions, we proposed self-consistency to evaluate the residues of each potential position. Only the top N_c potential locations with good self-consistency will retained to be used as input to the particle filter at time t.

B. Consistent Potential Position Generation

1) Historical Consistency: To avoid generating a large amount of misleading potential positions by blind combinations of the anonymous distances, we proposed to measure the *historical consistency* of the distances to narrow down their potential target IDs. The input of this step is the historical positions of the N targets and the distance set measured by the beacons. For a target, let v_e be the target's velocity upper bound in the real scenarios. Its position at round t will be bounded inside a disk centered at its position of round $t-1$, with radius $v_e\tau$, which τ is the time interval between two rounds.

$$\|\mathbf{x}_i(t) - \mathbf{x}_i(t-1)\| \leq v_e\tau \tag{6}$$

For a measured distance $D_{j,k}(t) \in \mathbf{D}_j(t)$ at beacon j, its initial potential transmitters include $\{1, \cdots, \text{or}, N\}$, which are called *target labels*. We reject the infeasible labels using the location consistence requirement in (6). Let's consider whether to accept or reject label i. Let $d_{j,i^{(t-1)}}$ be distance from beacon j to the target i's historical position $\mathbf{x}_i(t-1)$. From triangle inequality, if $D_{j,k}(t)$ is indeed measured from target i, since $\|\mathbf{x}_i(t) - \mathbf{x}_i(t-1)\| \leq v_e\tau$, there must be:

$$\left|D_{j,k}(t) - d_{j,i^{(t-1)}}\right| \leq v_e\tau \tag{7}$$

Therefore, we use this necessary condition (7) to narrow down the target labels for each measured distance. If (7) is satisfied, i is retained as a potential label of $D_{j,k}(t)$, otherwise i is confidently removed from the label set.

2) Potential Position Generation: After narrowing down target labels for the measured distances, each distance still has several retained potential labels. Then, for generating potential positions of a target i at round t, the distances with target label i will be selected to form a group. Let's denote the ith group contain Q_i distances. Then every $m \geq d+1$ distances from non-collinear beacons in the group will be combined to calculate a position for target i by using least square estimation algorithm. So that, at most $\sum_{m=3}^{Q_i} C(Q_i, m)$ positions can be generated for target i.

3) Self-Consistency: We further evaluate the self-consistency of the generated potential positions to further filter out the unreasonable position candidates. Considering a potential position $\mathbf{x}$ calculated by trilateration using distances $[D_1, \cdots, D_m]$ from beacons at location $\mathbf{z}_{b_1}, \cdots, \mathbf{z}_{b_m}$, the self-consistency of this location is measured by the residue of the location calculation:

$$S_x = \frac{1}{m}\sum_{i=1}^{m}\left(D_i - d_{x,b_i}\right)^2 \tag{8}$$

where d_{x,b_i} is the distance from $\mathbf{x}$ to beacon b_i. Then only top N_c potential positions with the best self-consistency performances will be retained as the input potential position of target i to be further processed by the particle filter at time t.

C. Probabilistic Particle Filter

The particle filter maintains following data structures:

1) l most possible tracks for each target up to time $t-1$, denoted by $\{\mathbb{T}_i(1:t-1) \in R^{l*(t-1)}\}$;
2) the probability distribution function (pdf) of each target's velocity, denoted by $p_v(x)$;
3) the probability distribution function of each target's acceleration, denoted by $p_a(x)$.

The pdfs of each target's velocity and acceleration are calculated based on historically velocity and acceleration up to $t-1$. They are utilized to evaluate the likelihood of the generated particles.

Generate and Evaluate Particles: For each target, say i, by connecting its l ending locations at $t-1$ (in its l tracks) to the N_c potential positions at time t, $l*N_c$ particles are generated, each particle represents a potential track. Then we evaluate the likelihood of each particle k, $k = 1, \cdots, l*N_c$ by the following likelihood function:

$$c_k = p_v\left(v_k(t)\right) p_a\left(a_k(t)\right) \tag{9}$$

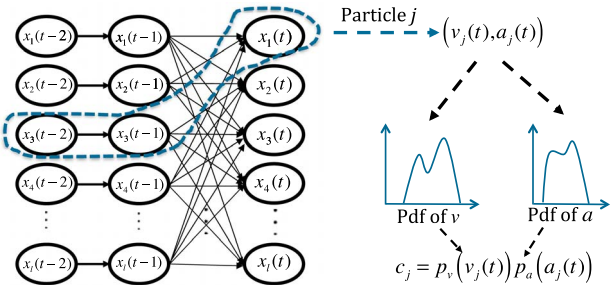

Fig. 10. Evaluate the cost of each generated particle.

where $v_k(t)$ and $a_k(t)$ are calculated on the particle k by:

$$v_k(t) = |\mathbf{x}_k(t) - \mathbf{x}_k(t-1)|, a_k(t) = v_k(t) - v_k(t-1). \quad (10)$$

The top l particles with best likelihood will be retained for the target for the next step, and $\mathbf{x}(t)$ in the most possible particle will be output as the position estimation at time t. The pdfs of velocity and acceleration are updated accordingly. Such a progress will be applied to all the targets, and the algorithm of the probabilistic particle filter is listed in Algorithm 2. Fig. 10 illustrates the principle of proposed probabilistic particle filter.

Algorithm 2 Probability Particle Filter for a Target i

Require: $\mathbb{T}_i(1:t-1)$, possible location $\{\mathbf{x}_1\mathbf{x}_2, \ldots, \mathbf{x}_{n_c}\}$. PDF of velocity $p_v(\cdot)$ and PDF of acceleration $p_a(\cdot)$.
Ensure: Updated $\mathbb{T}_i(1:t)$, $p_v(\cdot)$ and $p_a(\cdot)$, $\mathbf{x}_i(t)$.
1: $\{p_1, \ldots, p_{l\times n_c}\} \leftarrow \mathbb{T}_i(1:t-1) \times \{\mathbf{x}_1, \ldots, \mathbf{x}_{n_c}\}$ // Generate particles by possible locations of tracks at $t-1$
2: $\{c_1, \ldots, c_{l\times n_c}\} \leftarrow \mathbf{0}$
3: **for** $i = 1 : l \times n_c$ **do**
4: $v_k(t) = |\mathbf{x}_k(t) - \mathbf{x}_k(t-1)|$
5: $a_k(t) = v_k(t) - v_k(t-1)$
6: $c_k = p_v(v_k(t)) \cdot p_a(a_k(t))$
7: **end for**
8: $\{\hat{p}_1, \ldots, \hat{p}_{l\times n_c}\} \leftarrow$ sorting $\{p_1, \ldots, p_{l\times n_c}\}$ by $\{c_1, \ldots, c_{l\times n_c}\}$ in ascending order
9: $\mathbb{T}_i(1:t) \leftarrow \{\hat{p}_1, \ldots, \hat{p}_l\}$ // preserve the first l sorted particle
10: $p_a(\cdot) \leftarrow UpdatePDF(p_a(\cdot), \{v_1(t), \ldots, v_l(t)\})$
11: $p_v(\cdot) \leftarrow UpdatePDF(p_v(\cdot), \{a_1(t), \ldots, a_l(t)\})$
12: $\mathbf{x}_i(t) = \hat{p}_1$

Complexity of Algorithm 2 can be easily verified.

Lemma 1: Complexity of algorithm 2 is $O(NN_c l \log(N_c l))$

Proof 3: For each target, the most expensive step is to sort the $l * N_c$ elements, which takes $O(N_c l \log(N_c l)))$, so the overall complexity for locating the N targets is $O(NN_c l \log(N_c l)))$.

The probabilistic particle filter provides good flexibility. 1) It supports the trade off between the locating accuracy and the executing time by changing the number of the preserved particles. 2) The likelihood of each Particle is calculated by considering both the velocity and the acceleration, which is online continuously updated, so that it can be suitable even when the targets have variated motion characters.

A potential drawback of this particle filter approach is that a target may be lost when it is too close to other targets. When the location candidates of two targets are almost the same, all particles may follow one target and none particle follows the other. But this problem can be prevented in our approach by the location-based transmission scheduling scheme. The location-based transmission scheduling can avoid close targets transmitting together, which reduces the ambiguity in particle filter.

VII. Evaluation

Both simulations and experiments were conducted to evaluate the performances of multiple target locating in chorus mode. More specifically, *the locating accuracy, efficiency of scheduling and, the robustness of chorus locating against noise* were evaluated and reported in this section. More specifically, aforementioned collision model was implemented in simulation part. Simulation was conducted by Matlab 2013. In the simulation, several independent targets moving in 2D space, several receivers at fixed locations stood for beacons. Distance measurements from concurrent transmitting targets to the beacons were recorded in the form of matrix $[d_{i,j}]$, while $d_{i,j}$ was the range between beacon i to target j. Considering the characteristics of the NBU signal, i.e., anonymity, collision, attenuation and NLOS propagation, ToA measurement matrix $[d_{i,j}]$ was processed as follows.

1) *Anonymity*: Each row of $[d_{i,j}]$ was sorted in ascending order, such that $d_{i,j}$ was the jth large range to receiver i. The association between index and identity of target was erased.
2) *Collision*: $d_{i,j}$ was set to invisible if $\exists d_{i,k}$, such that $0 < d_{i,j} - d_{i,k} < \omega$.
3) *Attenuation*: $d_{i,j}$ was set to invisible if $d_{i,j} > R$.
4) *NLOS propagation*: A random positive matrix $[\upsilon_{i,j}]$ was added to $[d_{i,j}]$, where υ was i.i.d. random variable with uniform distribution to simulate the ranging noise.

The collision distance ω and the length of NLOS noise is important in simulation. Primary experiment was performed before simulation to learn ω. The value of NLOS noise was measured in our previous work [20], which can be resolved by sensor fusion algorithms [10], [15].

A. Primary Experiment for ω's Distribution

To measure ω, 4 targets and 1 receiver were used and the length of ω was measured by Oscilloscope. Oscilloscope was set to capture the rising-edge and lasting time of the received ultrasound signal. The width of signal over a threshold was captured as ω. In the first experiment, one target was scheduled to send signal periodically. In the second experiment, four targets were scheduled to work in chorus mode. The width distribution of ω captured by the receiver were shown in Fig. 11.

When one target was transmitting, ω distributed mainly within $[0, 1]$. The distribution is like a normal distribution,

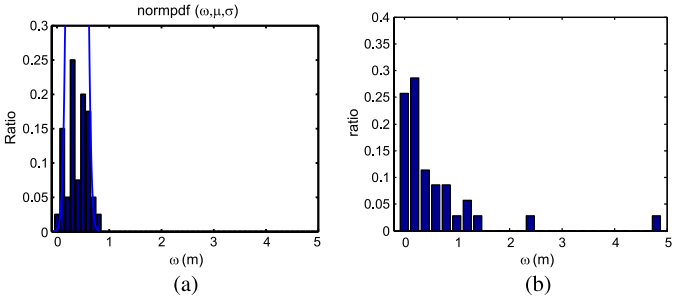

Fig. 11. Distribution of aftershock. (a) Distribution of aftershock by one target. (b) Distribution of aftershock by 4 targets.

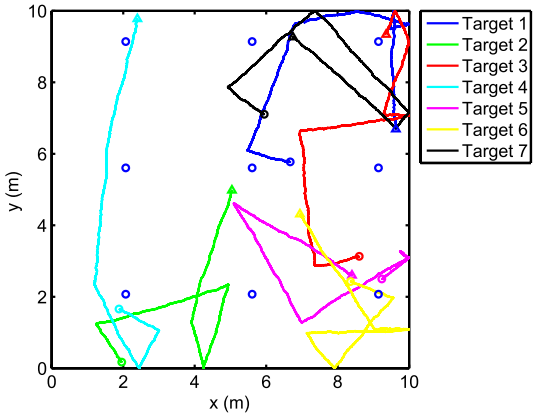

Fig. 12. Setting of simulation.

with $\mu = 0.5$ and $\sigma = 1$. When 4 targets worked concurrently, *omega* increased because of the inevitable signal interference. In this case, the major distribution was within [0, 1.5 m]. We used these parameters in simulation.

B. Simulation

1) Settings of Simulation: Multi-agent simulation was conducted in MATLAB. Each target conducted random walk independently in 2-dimensional space, with parameter settings like human being's. The parameters included velocity, specified by mean value $\mu_v = 2$ m/s and deviation $\sigma_v = 1$ m/s, the interval between turning, the time between turning, and the turning angle. Receivers were deployed at intersection of grid, whose unit size was 3 m × 3 m. Simulation proceeded in constant step, 1 ms. In every step, location of every target was updated. Fig. 12 showed the deployment of receivers and the examples of the targets' trajectories. The triangles stood for the start points and circle stood for the end points. In simulation, these trajectories were used as ground-truth, with which the locating error could be calculated.

Fig. 13 shows the ranges obtained in exclusive mode and chorus mode in simulation at the receivers part. Upper sub-figure shows the ranges obtained in exclusive mode and the lower sub-figure shows that obtained in chorus mode. The bar clustered at a receiver R_i stands for the range obtained by the receiver i. We can see that in chorus mode, fewer ranges were obtained due to the collision and the identities of ranges were lost, indicated by the single color of the bars. The codes and simulation setting are hosted in the following public repository for open access. (https://bitbucket.org/thufresh/multipletargetscheduling).

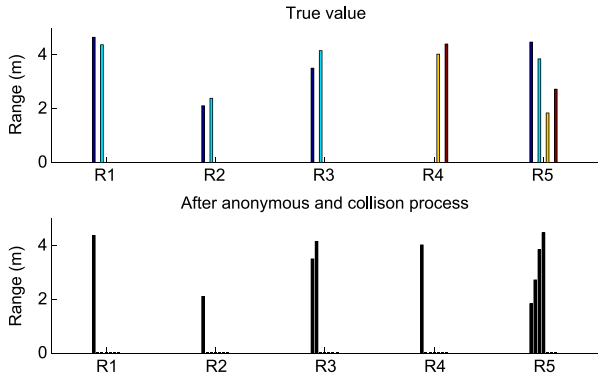

Fig. 13. Range obtained by receivers.

2) Tracking Fidelity: The most significance of chorus locating is that the targets can be located in high refreshing rate, which is useful especially when trajectory of targets contain sharp turns. To validate this fact, the same trajectories were tracked in both exclusive and chorus modes. Tracking results of two different modes were compared from several aspects. In chorus mode, ω was assigned to 0.5 meter, which is the averaged value obtained in primary experiment. In both the chorus mode and the exclusive mode, the locating time slot was set to 100 ms, which was used in Dragon [20] and Cricket [14].

Fig. 14(a)–(c) show the locating results in exclusive and locating in chorus mode respectively. In general, the ground-truth of each trajectory is a piece-wise linear curve plus slight swings. The tracking results in exclusive mode were smoother than the ground-truth, which was caused by the low refreshing rate. The slight swings and sharp turns were lost in the exclusive mode. The tracking results obtained in chorus mode were more sharp. The sharp turns could be seen in the tracking results. The side effect is that, some locating errors are presented at the straight lines. The difference could be seen clearly by zooming into a specific trajectory, for example, the black one. Let's focus on two parts in the trajectory, which are denoted by the blue and red circles. In the part denoted by the red circle, sharp turn happens. Tracking result in chorus mode can follow the ground-truth well due to the higher refreshing rate. In the same area, the exclusive mode fails to follow the sharp turn due to the big interval between the location update. While in the blue circuit area, chorus mode has big locating error, which may be caused by the shortage of range because of collision. By comparing the locating result in chorus mode with the ground-truth point-by-point, the locating error in chorus mode can be counted. Linear interpolation was performed on the chorus locating result to make its spatial resolution equal to the ground-truth. Tracking error in exclusive mode was obtained in the same way. The cumulated distribution of the locating error of two mode are contrasted in Fig. 14. Obviously, the tracking accuracy obtained in chorus mode is slightly better. Not that in the comparison, no ranging error is introduced. The robust of chorus locating was tested in the following subjects.

3) Tracking Accuracy Over NLOS Noise and Collision: In chorus locating, collision may caused by shortage of ranges, which results in location failure. When range measurement is degenerated by NLOS error, the locating result may get even worse. How the collision and noise affects the accuracy of locating is revealed in this subject.

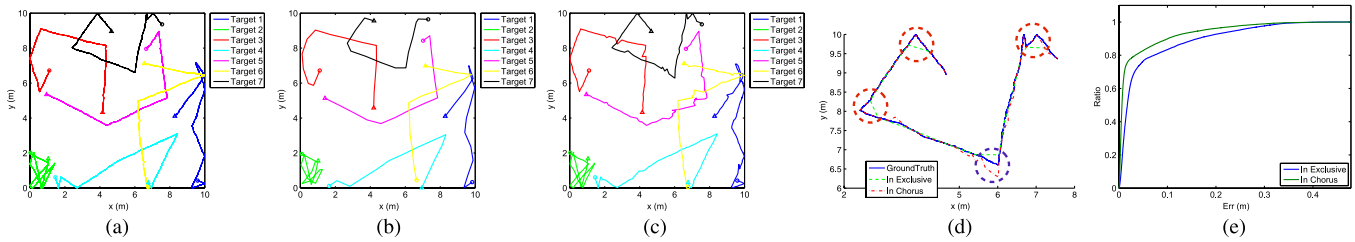

Fig. 14. Tracking fidelity contrast between chorus mode and exclusive mode. (a) Ground-truth. (b) In exclusive mode. (c) In chorus mode. (d) Zoom-in for detail. (e) CDF.

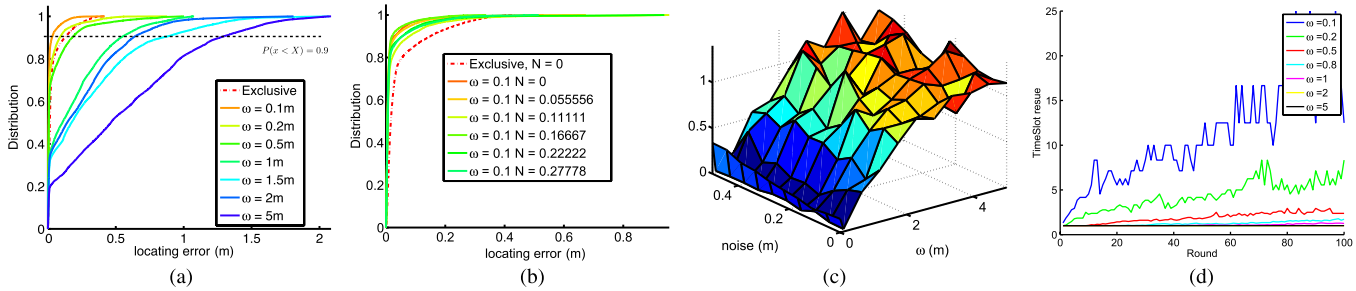

Fig. 15. Robustness and efficiency of chorus locating. (a) CDF vs ω. (b) CDF vs. noise. (c) Locating accuracy over both Noise and ω. (d) Timeslot reuse changes with ω.

The setting of simulation was the same as in the previous subject. To reveal the effect of collision, the length of ω was changed from 0.5 m to 5 m, The maximum NLOS noise was also increased from 0 to 50cm. For each combination of these two parameters, CDF of locating error was calculated.

CDF of locating error obtained with different ω is shown in Fig. 15(a). The locating error obtained in the exclusive mode is denoted by the dashed line, while CDF with chorus mode is denoted by the solid line. The black broken line illustrated the position of 90% ratio. The 90% line is intersected by every curve, while the x-coordinate of the intersection spot indicates the locating accuracy. In general, the locating accuracy decreased with ω from centimeter level to about 1 m. In particular, when ω is less than 0.2 meter, the locating accuracy is better than the exclusive mode. Referring to Fig. 11(b), the majority of ω is smaller than 1 meters in practice, such that we can expect the locating accuracy in less than 1 meter.

When NLOS error in introduced, locating accuracy is degenerated. In practical system, such as Dragon and Cricket, NLOS is introduced by the reflection propagation on the wall, ceiling and facilities nearby, therefore the NLOS error varied in different environment. Experiment in Dragon shows that the ranging error is distributed over $[0, 0.5\text{ m}]$. In our simulation, the same range error distribution was applied to the ranging measurement. Fig. 15(b) shows that the locating error was not sensitive to the change of the NLOS noise. The reason is because of the Least Square Estimation, which reduce the NLOS effect in certain degree.

The location accuracy distribution over both ω and the NLOS noise is illustrated in Fig. 15(c). Each vertex $(\omega, \mathcal{N}, z)$ on the surface means that the locating accuracy is z under collision length ω and noise length $\mathcal{N}$. It is noted that, when $\omega = 0$, we use exclusive locating other than chorus locating. An remark of Fig. 15(c) is that the locating accuracy is more sensitive to ω other than noise. This remark indicates the importance of LBTA scheduling protocol, which can reduce the probability that collision happens.

4) Performance of LBTA: Chorus locating allows multiple targets to be located in one time-slot. The number of targets located in one time-slot, denoted by n_u was referred as *time-slot reuse ratio*. In exclusive mode, $n_u = 1$ is constant. In chorus locating, n_u is a variable, which is determined by the scheduling algorithm. Experiments in simulation showed how n_u changed in the locating process and how n_u was affected by ω. When 50 targets were deployed in 10 m $\times$ 10 m 2D space, chorus locating was performed in every 100ms interval. n_u for the first 200 locating round was recorded.

As shown in Fig. 15(d), for every ω, n_u equals to 1 initially and increased gradually with the locating process. This is because the LBTA initialized each un-located target with an exclusive time-slot. As the locating process continued, the number of un-located target reduced. As LBTA increased the transmitting concurrency, the time-slot reuse ratio increased. But if ω increased, less concurrent transmitters can be scheduled. We can see the time-slot reuse ratio decreased with ω.

C. Testbed Experiment

We developed testbed systems to verify the proposed chorus mode ranging and chorus mode locating methodologies. Experiments were conducted in two systems: one is composed by wireless targets and wireless receivers, called *wireless system*; another is our previously developed *Dragon system* [20], in which the receivers are connected by cables.

The Wireless System: In the wireless system, targets and receivers were implemented by the Cricket [14] node. The difference from the Cricket system is that the targets in our system don't broadcast RF signal for time synchronization. Instead, an external wireless commander works as *synchronizing commander* to broadcast RF to all receivers and targets. Each

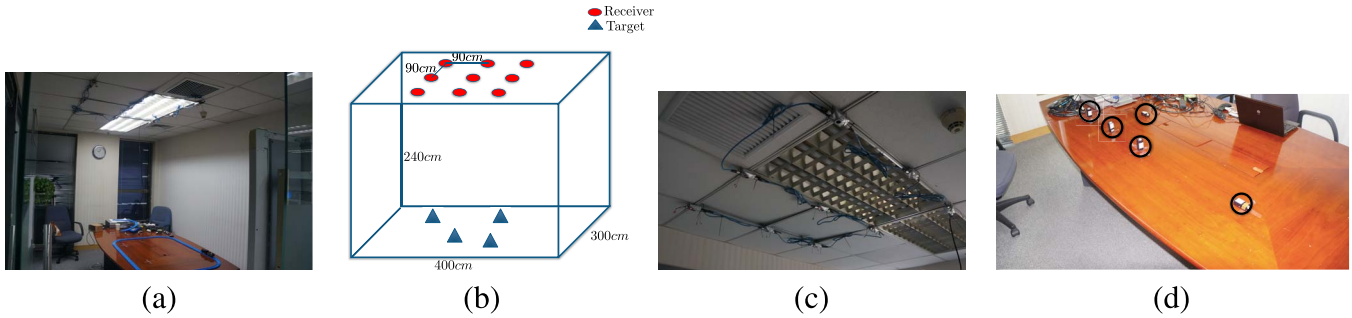

Fig. 16. Setting of test-bed. (a) Room of experiment. (b) Dimension and Setting. (c) Receivers. (d) Targets.

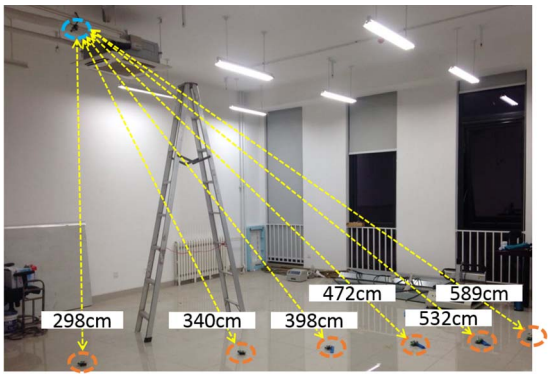

Fig. 17. Setting of chorus mode ranging experiment.

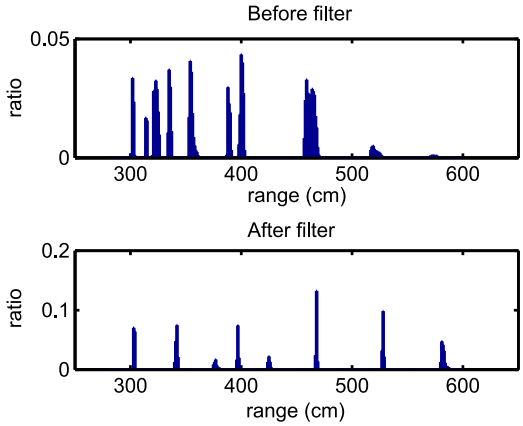

Fig. 18. Histogram of distance measurements with and without NLOS filter.

target broadcasts ultrasound pulse immediately after receiving the RF signal. Each receiver starts its clock to wait for the ultrasound pulse after receiving the synchronization signal. It records timestamps of all captured ultrasound pulses, and reports these captured timestamps to the base station at the end of an locating interval, i.e., 50 ms.

The Dragon System: Because each receiver need to report the capturing timestamps of a large set of ultrasound pulses (including echoes and NLOS detections, which contribute more than 100bytes) to the base node, the slow wireless links of Cricket could not afford reliable data transmission within the locating interval because of the interference among the multiple receivers in the locating experiment. Therefore, the wireless system is mainly used in chorus ranging experiments for the flexibility of generating different target-receiver distances. A Dragon [20] system, which connected all US receivers by cable was used in chorus mode locating. In Dragon system, there were totally 9 receivers, as shown in Fig. 16. In Dragon, the receivers transmitted their captured data efficiently using the wired links without the wireless interference.

1) Chorus Mode Ranging: We firstly investigated the chorus mode ranging efficiency and accuracy using the wireless system. A receiver was hanged at 3 meters high on the ceiling. Six targets were deployed alone a line on the floor. The deployment scenario is shown in Fig. 17. The geometric relationship among the receiver and the targets is illustrated in the Fig. 17. Based on the timestamps captured the receiver, distance set measured by the receiver were calculated and compared with the ground truth. The top subfigure of Fig. 18 showed the histogram of the detected distance set by the receiver in 100 times of experiments. We can see that more than six distances were frequently measured, because effects of the echoes and the NLOS pulses. To filter out the NLOS pulses, an energy-based filter was applied to filter out the ultrasound pulses whose detected energy was less than a threshold, because the echoes and reflections generally had smaller energy than the direct-path pulses. The bottom subfigure in Fig. 18 showed the histogram of the detected distance set when a NLOS filter was applied. The histogram shows that the six distances were generally detected correctly and reliably. It shows the high efficiency of chorus mode locating.

2) Efficiency of Chorus Mode Locating: Chorus mode locating experiments were conducted by Dragon system, in which four targets were used and the Dragon system contained nine receivers. At first, the signals from four concurrent transmitters captured by nine beacons at different locations were shown in Fig. 19. We can see that the signals captured by the beacons at different locations were different greatly. At beacons 3, 4 and 9, exactly four rising edges were captured. At location 1, 7, 5 and 8, the number of rising edge was less than four. Several TOA measurements were lost due to the signal collision. The length of after shock was obviously longer than the non-collision case. At the rest locations, we can see the beacons captured more than four rising edge, which was caused by the NLOS propagation. The NLOS effects were reduced by applying energy-based filter and COFFEE algorithm [20]. The key idea is that the ranges generated by NLOS can not consist with correct range in the triangulation process which will be filtered out.

In locating experiments of the four targets, one target was attached to a pedestrian, who moved around the table. Another target was attached on a toy train, which moved automatically along round-rectangle track as shown in Fig. 16. The other two

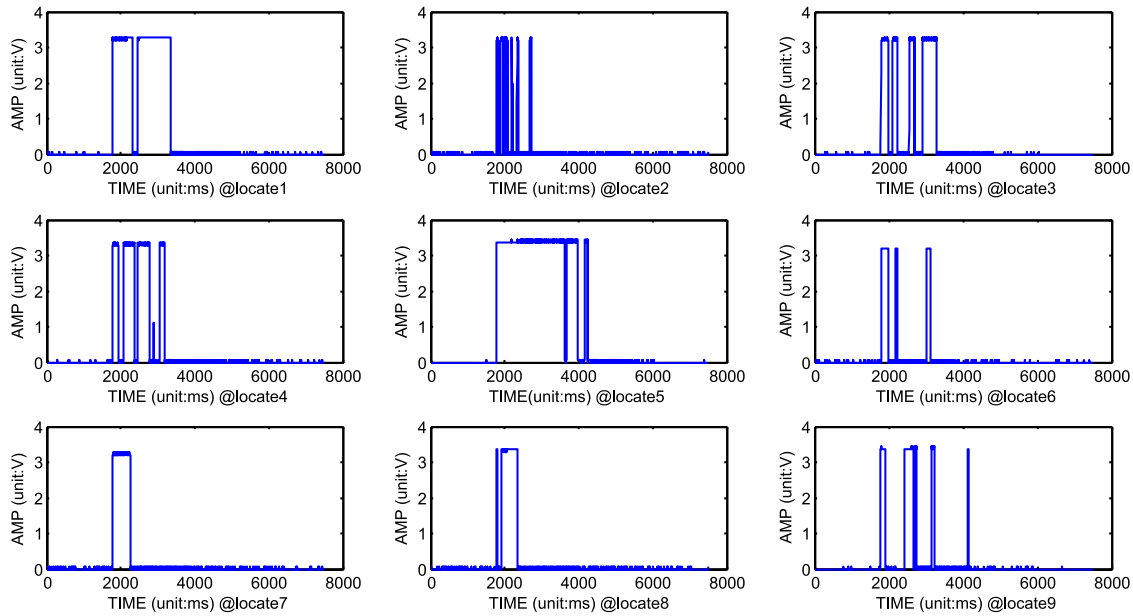

Fig. 19. Signal captured by 9 receiver.

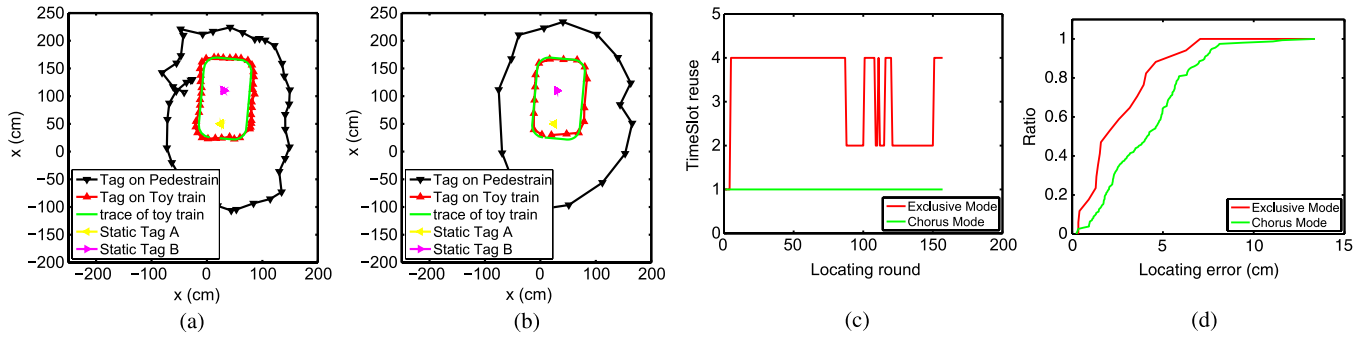

Fig. 20. Evaluating chorus locating in testbed. (a) Locating 4 targets in chorus mode. (b) Locating 4 targets in exclusive mode. (c) Contrast on timeslot reuse. (d) Contrast on locating accuracy.

targets were placed on table, which were static. The location tracking results for the four targets in chorus and exclusive modes were shown in Fig. 20. The traces of four targets were illustrated by dot-lines of different colors. Each dot stands for an obtained location. The track of the toy train was drawn in the picture as the ground truth.

According to Fig. 20, the locations obtained by chorus mode locating is much denser than that obtained in exclusive mode. More specifically, we evaluated the time slot reuse ratio. The results were compared in Fig. 20(c). In exclusive mode, the time-slot reuse ratio is always 1. But in chorus mode, the time-slot reuse is 4 in most locating round.

3) Tracking Accuracy: To evaluate the tracking accuracy, the locating results were compared with the ground-truth. Since the ground truth of the pedestrian is hard to obtain, we only evaluated the locating error for tracking static targets and the toy train. In Fig. 20, we can see that the locating results matched the ground truth well in both modes. The cumulated distribution function of locating error was illustrated in Fig. 20(d). It showed that the tracking accuracy obtained by chorus locating was as good as that obtained in exclusive mode locating. In general, the testbed experiments verified the fact, that locating in chorus could provide promising accuracy and much higher location updating rate than the traditional exclusive mode TOA-based locating.

VIII. Conclusion

In this paper, we have investigated how to locate multiple narrowband ultrasound targets in chorus mode. It is to allow the targets broadcast ultrasound concurrently to improve the position updating rate, while disambiguating their locations by algorithms at the receiver end. We investigated the geometric conditions among the targets for confidently separating the NBU waves at the receivers, and the geometrical conditions for obtaining at least $d+1$ distances for each concurrent target. To deal with the anonymous distance measurements, consistent position generation and probabilistic particle filter algorithms were presented to label potential sources for anonymous distances and to disambiguate the trajectories of the multiple concurrent targets. To avoid conflicts of the close by targets and for reliable initialization, a location based concurrent transmission scheduling algorithm was developed. Simulations and experiments showed the feasibility and efficiency of chorus mode locating. Further work may includes more flexible wavefront detection technique to further shorten the aftershock; and detection methods to be more robust to echoes and noises.

APPENDIX

A. Expression of Equation (2)

where

$$\theta = \arccos \frac{d_{a,b}}{2r} \tag{11}$$

and

$$S_e = \int_0^{y_\beta} \left(2\sqrt{r^2 - y^2} - \omega v_u \sqrt{1 + \frac{y^2}{d_{a,b}^2 - \frac{1}{4}\omega^2 v_u^2}} \right) dy \tag{12}$$

where

$$y_\beta = \frac{b_h}{c_h} \sqrt{r^2 - b_h^2 - 2a_h r} \tag{13}$$

refers to the y coordination of intersection point of hyperbola and circle.

$$a_h = \frac{v_u \omega}{2}, \quad b_h = \frac{d_{a,b}}{2}, \quad c_h = \sqrt{a_h^2 + b_h^2} \tag{14}$$

REFERENCES

[1] M. Alloulah and M. Hazas, "An efficient CDMA core for indoor acoustic position sensing," in *Proc. IPIN*, 2010, pp. 1–5.

[2] W. Choi, A. Forenza, J. Andrews, and R. Heath, "Opportunistic space-division multiple access with beam selection," *IEEE Trans. Commun.*, vol. 55, no. 12, pp. 2371–2380, Dec. 2007.

[3] A. V. Fishkin, "Disk graphs: A short survey," in *Approximation and Online Algorithms*, Berlin, Germany: Springer-Verlag, Jan. 2004, 1–5.

[4] J. Gonzalez Hernandez and C. Bleakley, "Accuracy of spread spectrum techniques for ultrasonic indoor location," in *Proc. 15th Int. Conf. Digit. Signal Process.*, Jul. 2007, pp. 284–287.

[5] J. Gonzalez Hernandez and C. Bleakley, "High-precision robust broadband ultrasonic location and orientation estimation," *IEEE J. Sel. Topics Signal Process.*, vol. 3, no. 5, pp. 832–844, Oct. 2009.

[6] J. Gonzalez Hernandez and C. Bleakley, "Low-cost, wideband ultrasonic transmitter and receiver for array signal processing applications," *IEEE Sensors J.*, vol. 11, no. 5, pp. 1284–1292, May 2011.

[7] A. Gore, A. Karandikar, and S. Jagabathula, "On high spatial reuse link scheduling in STDMA wireless ad hoc networks," in *Proc. IEEE GLOBECOM*, Nov. 2007, pp. 736–741.

[8] M. Hazas and A. Hopper, "Broadband ultrasonic location systems for improved indoor positioning," *IEEE Trans. Mobile Comput.*, vol. 55, no. 5, pp. 536–547, May 2006.

[9] M. Hazas and A. Ward, "A novel broadband ultrasonic location system," in *UbiComp 2002: Ubiquitous Computing*, G. Borriello and L. E. Holmquist, Eds., vol. 2498, Lecture Notes in Computer Science, Berlin, Germany: Springer-Verlag, Jan. 2002. 264–280.

[10] S. Iyengar and R. R. Brooks, *Distributed Sensor Networks*, 2nd ed. ser. Image and Sensor Signal Processing Series, London, U.K., Chapman & Hall, 2012.

[11] L. Lu, H.-C. Wu, and S. S. Iyengar, "A novel robust detection algorithm for spectrum sensing," *IEEE J. Sel. Areas Commun.*, vol. 29, no. 2, pp. 305–315, Feb. 2011.

[12] M. Minami *et al.*, "DOLPHIN: A practical approach for implementing a fully distributed indoor ultrasonic positioning system," in *UbiComp 2004: Ubiquitous Computing*, vol. 3205, N. Davies, E. D. Mynatt, and I. Siio, Eds., Lecture Notes in Computer Science, Berlin, Germany: Springer-Verlag, Jan. 2004, pp. 347–365.

[13] A. Nishitani, Y. Nishida, T. Hori, and H. Mizoguchi, "Portable ultrasonic 3d tag system based on a quick calibration method," in *Proc. IEEE Int. Conf. Syst., Man Cybern.*, Oct. 2004, vol. 2, pp. 1561–1568.

[14] N. B. Priyantha, A. Chakraborty, and H. Balakrishnan, "The Cricket location-support system," in *Proc. 6th Annu. Int. Conf. MobiCom Netw.*, Aug. 2000, pp. 32–43.

[15] R. R. Brooks and S. S. Iyengar, *Multi Sensor Fusion—Theory and Practice*. Upper Saddle River, NJ, USA: Prentice-Hall, 1998.

[16] M. M. Saad, C. J. Bleakley, and S. Dobson, "Robust high-accuracy ultrasonic range measurement system," *IEEE Trans. Instrum. Meas.*, vol. 60, no. 10, pp. 3334–3341, Oct. 2011.

[17] H. Schweinzer and G. Kaniak, "Ultrasonic device localization and its potential for wireless sensor network security," *Control Eng. Pract.*, vol. 18, no. 8, pp. 852–862, Aug. 2010.

[18] L. Song and Y. Wang, "Locating multiple ultrasound targets in chorus," in *Proc. IEEE Int. Conf. SECON*, Singapore, Jun. 2014, pp. 99–107.

[19] J. Villadangos *et al.*, "Improvement of ultrasonic beacon-based local position system using multi-access techniques," in *Proc. IEEE Int. Workshop Intell. Signal Process.*, Sep. 2005, pp. 352–357.

[20] Y. Wang and L. Song, "An algorithmic and systematic approach for improving robustness of TOA-based localization," in *Proc. IEEE 10th Int. Conf. HPCC-EUC*, 2013, pp. 2066–2073.

[21] Y. Wang, J. Zhao, and T. Fukushima, "LOCK: A highly accurate, easy-to-use location-based access control system," in *Location and Context Awareness*, vol. 5561, Lecture Notes in Computer Science, Berlin, Germany: Springer-Verlag, 2009, pp. 254–270.

[22] A. Ward, A. Jones, and A. Hopper, "A new location technique for the active office," *IEEE Pers. Commun.*, vol. 4, no. 5, pp. 42–47, Oct. 1997.

[23] O. Woodman and R. Harle, "Concurrent scheduling in the active bat location system," in *Proc. 8th IEEE Int. Conf. PERCOM Workshops*, Mar. 2010, pp. 431–437.

[24] U. Yayan, H. Yucel, and A. Yazc, "A low cost ultrasonic based positioning system for the indoor navigation of mobile robots," *J. Intell. Robot. Syst.*, vol. 78, no. 3/4, pp. 541–552, Jun. 2015.

[25] H. Yin and H. Liu, "Performance of space-division multiple-access (SDMA) with scheduling," *IEEE Trans. Wireless Commun.*, vol. 1, no. 4, pp. 611–618, Oct. 2002.

[26] J. Zhao and Y. Wang, "Autonomous ultrasonic indoor tracking system," in *Proc. ISPA*, 2008, pp. 532–539.

[27] J. Zhao and Y. Wang, "Pospush: A highly accurate location-based information delivery system," in *Proc. UBICOMM*, 2009, pp. 52–58.

Yongcai Wang (M'11) received the B.Sc. and Ph.D. degrees from Tsinghua University, Beijing, China, in 2001 and 2006, respectively. From 2007 to 2009, he was an Associate Researcher with NEC Labs China. From 2009 to 2011, he was a Postdoctoral Fellow with the Institute for Interdisciplinary Information Sciences, Tsinghua University, where he has been an Assistant Researcher since 2011. From February 2014 to August 2014, he was a Visiting Scholar with Cornell University. His major research interests lie in the broad area of sensor networks, network measurement, and wireless locating algorithms and systems. He was a recipient of the best paper awards at Ubicomm2009 and CWSN2011.

Lei Song (S'12–M'14) received the B.Sc. degree from Tsinghua University, Beijing, China, in 2007 and the M.S. degree from the Institute of Computing Technology Chinese Academy of Sciences, Beijing, in 2010. He is currently working toward the Ph.D. degree in the Institute for Interdisciplinary Information Sciences, Tsinghua University. His research interests mainly include wireless sensor network and indoor locating and system.

S. S. Iyengar (F'95) is currently the Ryder Professor of Computer Science and the Director of the School of Computing and Information Sciences at Florida International University, Miami, FL, USA. He has authored or coauthored over 400 research papers and eight books and has edited 12 books. He has been involved with research in high-performance algorithms, data structures, sensor fusion, data mining, and intelligent systems. He is a member of the European Academy of Sciences and the Institute of Electrical and Electronics Engineers (IEEE) Golden Core and a Fellow of the IEEE, the Association of Computing Machinery, the American Association for the Advancement of Science, and the Society for Design and Process Science. He was a recipient the Distinguished Alumnus Award of the Indian Institute of Science and the IEEE Computer Society's Technical Achievement Award in 1998.